PHYSICAL REVIEW B VOLUME 14, NUMBER 1 1 JULY 1976

Specific heats of paraelectrics, ferroelectrics, and antiferroelectrics at low temperatures

W. N. Lawless
Corning Glass Works, Research Laboratory, Corning, New York 14830
(Received 1 March 1976)

Measurements of low-temperature specific heats (2–37 K) are reported for the first time on some common paraelectrics (thallous halides, PbF_2, $KTaO_3$), ferroelectrics [$BaTiO_3$, potassium dihydrogen phosphate or KDP, triglycine sulfate or TGS, $LiNbO_3$, $LiTaO_3$, $Pb(Zr_{0.65}Ti_{0.35})O_3$ or PZT 65/35], and antiferroelectrics [$Pb(Zr_{0.95}Ti_{0.05})O_3$ or PZT 95/5, $Pb_2Nb_2O_7$]. All materials display maxima in CT^{-3}, and excellent fits to experimental data are obtained with single Einstein frequencies. The Einstein frequencies vary from 19 cm^{-1} for TlCl to 99 cm^{-1} for $BaTiO_3$. The frequencies in $LiNbO_3$ (79 cm^{-1}) and $LiTaO_3$ (61 cm^{-1}) agree reasonably well with earlier Raman data at 300 K on E-symmetry optic modes and with recent low-temperature pyroelectric data. The TlBr frequency (22 cm^{-1}) agrees well with the lowest phonon anomaly determined from neutron data, and the $KTaO_3$ frequency (26 cm^{-1}) is in good agreement with the average soft-mode frequency in this temperature range. No evidence is seen for the suggested phase transition in $KTaO_3$ at 10 K. The PZT materials, which are compositionally in a field inaccessible to powder Raman methods, have frequencies of 32 (65/35) and 38 cm^{-1} (95/5), due probably to low-lying TA phonons. An unusual $T^{3/2}$ contribution to the specific heat of the ferroelectrics TGS, KDP, $BaTiO_3$, and $LiNbO_3$ was found at the lowest temperatures. Experimental data are in excellent agreement with $C = AT^3 + BT^{3/2}$, and it is suggested that the $T^{3/2}$ term is the domain-wall contribution.

I. INTRODUCTION

Low-lying vibrational modes are known to play an important role in the properties of amorphous, superconducting, and ferroelectric materials. The measurement of low-temperature thermal properties is one method of sampling these modes since the higher modes are depopulated. A case in point is vitreous SiO_2, where low-frequency modes (~30 cm^{-1}) are responsible for the plateau region in the thermal conductivity at about 10 K and for the anomalous specific heat, which is larger than that predicted from elastic-wave velocities.[1]

A low-frequency mode is often described by an Einstein specific-heat term added to the Debye term, and it is straightforward to show that if $T \ll \Theta_D$, CT^{-3} will have a maximum at $T_{max} \simeq \nu_E/3$, where ν_E is the Einstein frequency (in cm^{-1}). This simple example shows that low-lying modes in the range ~5–100 cm^{-1} should be manifested in specific-heat measurements in a convenient range of low temperatures.

Einstein modes between 26 and 49 cm^{-1} have recently been found from specific-heat measurements on the superconducting hexagonal tungsten bronzes.[2] These modes dominate the specific heats of these bronzes at low temperatures and are attributed to metal ions vibrating in the channels formed by the WO_6 octahedra. Similarly, phonon anomalies in the superconductor TaC have recently been studied calorimetrically (the transition temperature was magnetically suppressed).[3] An Einstein mode $\nu_E \cong 107$ cm^{-1} was found which agreed well with a calculated van Hove singularity in the density of states.[4]

Low-lying modes in ferroelectrics have received considerable attention over the past ten years following the introduction of the soft-mode concept by Cochran.[5] The notion here is that an optic-mode frequency softens—decreases with decreasing temperature—and extrapolates to zero in the neighborhood of the ferroelectric phase transition. Soft modes have now been observed by neutron and light scattering experiments in several ferroelectrics, antiferroelectrics, and paraelectrics.[6] The mode can then be low lying at temperatures below the phase transition.

The thermal properties of ferroelectrics at low temperatures have received scant attention. The specific heats of the thallous halides (which are paraelectrics) have been measured, but only at temperatures above 5 K and at too widely spaced temperatures to resolve Einstein modes.[7] Hegenbarth[8] has reported specific-heat data on $SrTiO_3$ between 20 and 80 K, and the specific heat of lithium sulfate monohydrate has been reported over the range 13–300 K.[9]

The purpose of this paper is to report new low-temperature specific-heat data in the range 2–37 K on some well-known paraelectrics (thallous halides, PbF_2, $KTaO_3$), ferroelectrics ($BaTiO_3$, triglycine sulfate or TGS, potassium dihydrogen sulfate or KDP, $LiNbO_3$, $LiTaO_3$, $PbZr_{0.65}Ti_{0.35}O_3$ or PZT 65/35) and antiferroelectrics ($Pb_2Nb_2O_7$, $PbZr_{0.95}Ti_{0.05}O_3$ or PZT 95/5). As will be seen below, all of these materials display large specific heats at low temperatures due to low-

lying modes with frequencies in the range from 19 to 100 cm^{-1}. As was found with the tungsten bronzes mentioned above, these Einstein modes dominate the phonon spectra at low temperatures.

The ferroelectrics measured show an additional feature in the specific heat at temperatures low enough to freeze out the Einstein oscillators, and it is suggested that this may be due to the domain-wall contribution.

II. EXPERIMENTAL METHOD AND RESULTS

Specific-heat data were measured in a pulse calorimeter designed to accomodate large voltages for electrocaloric measurements also. Consequently, neither a sample holder nor helium exchange gas was used. Each sample was fixured with a heater (~150 Ω) and a machined carbon resistor (220-Ω, $\frac{1}{8}$-W Allen Bradley) using GE 7031 varnish. A manganin wire (0.0125 cm diam) varnished to the sample and indium soldered to the reservoir served as the thermal link, and the lengths of these links were chosen to give time constants ~100 sec at 2 K (much larger time constants were involved at higher temperatures). Portions of the carbon thermometer leads (0.002-cm-diam manganin) were tempered to the sample, and both heater and thermometer leads were thermally anchored to the reservoir.

The addenda were determined by cumulative weighings (~±0.2 mg) and constituted (2–7)% by weight. Lead lengths between the sample and reservoir were included in the addenda, and the heater resistance was corrected for the power flow in the heater leads between the sample and reservoir.[10] Addenda corrections were made using literature tabulations for the metals and graphite[11] and varnish.[12]

The reservoir (adiabatic shield) was a copper can outfitted with heater coils and a silicon diode thermometer and controlled by a Lake Shore Cryotronics model DTC-500 temperature controller. The reference thermometer was a calibrated germanium thermometer[13] bolted into the lid of the reservoir. The thermal link was indium soldered to the lid of the reservoir can, and the reservoir in turn was suspended on copper straps from the flange of an immersion cryostat. Charcoal granules were placed in the bottom of the cryostat, and the vacuum spaces of the cryostat and reservoir can were connected by drill holes. Two samples per run were accommodated, and the samples could be pulsed independently.

The sample thermometry was handled as follows: Experience with the 220-Ω, $\frac{1}{8}$-W carbon thermometers showed that in the temperature range of interest, the expression

$$\log_{10}R = A + BT^{-P} \tag{1}$$

describes the R-T characteristic very well. Typically, the fitting index of regression is ≥ 0.9999 and the residual standard deviation $\simeq 10$ mK ($A \simeq 2.37, B \simeq 3.47, P \simeq 0.78$). The carbon thermometer was calibrated *in situ* during the course of the run by taking about 15 points and fitting the R-T data to Eq. (1) using nonlinear regression-analysis methods. Bringing the sample and reservoir into equilibrium for a calibration point through the long-time-constant link was facilitated by balancing the sample heater and the reservoir heater.

The remaining details were standard calorimetric methods. Heat pulses of 3–10-sec duration were applied after the sample and reservoir were in approximate equilibrium, and the temperature rise and slow drift back to the reservoir temperature were monitored on a strip-chart recorder. Temperature rises $\Delta T/T$ were maintained at (3–5)%. The uncertainty in the method is believed to be $< \pm 5\%$ based on measurements of fused silica.[14]

Single crystals of TlCl (0.2494 g), TlBr (0.5543 g), PbF_2 (0.8341 g), $KTaO_3$ (0.4204 g), $BaTiO_3$ (1.2140 g), $LiNbO_3$ (0.8808 g), $LiTaO_3$ (1.4056 g), TGS (0.4943 g), and KDP (0.5096 g) were measured. In the case of $BaTiO_3$, several large butterfly twins were varnished together. The remaining samples were ceramics of TlI (0.4845 g), PZT 65/35 (1.4301 g), PZT 95/5 (1.1213 g), and $Pb_2Nb_2O_7$ (1.0303 g).

The range of addenda heat capacities expressed as a percentage of the total heat capacity were as follows: TlCl, (3–9)%; TlBr, (2–9)%; PbF_2, (4–18)%; TlI, (3–8)%; $KTaO_3$, (9–24)%; $BaTiO_3$, (7–32)%; $LiNbO_3$, (15–40)%; $LiTaO_3$, (14–80)%; TGS, (3–14)%; KDP, (3–14)%; PZT 65/35, (3–16)%; PZT 95/5, (4–11)%; and $Pb_2Nb_2O_7$, (10–30)%. The addenda contributions were largest at the lowest temperatures owing to the electronic term in the specific heat of the metals. For this reason the literature data[11] were carefully curve fitted for use in the data reduction.

The measured data on these materials are shown in Figs. 1–5. The CT^{-3}-vs-T^2 semilog plots were chosen as a very sensitive way to display the CT^{-3} maxima.

All materials have CT^{-3} maxima which vary from ~5 K for TlCl to ~27 K for $BaTiO_3$, suggesting Einstein modes in the range ~15–100 cm^{-1}. The strengths of these modes appear strongest for TlCl and weakest for $LiNbO_3$.

The *ferroelectric* materials in Figs. 3 and 4 show an additional feature—namely, an increase in CT^{-3} with decreasing temperature at tempera-

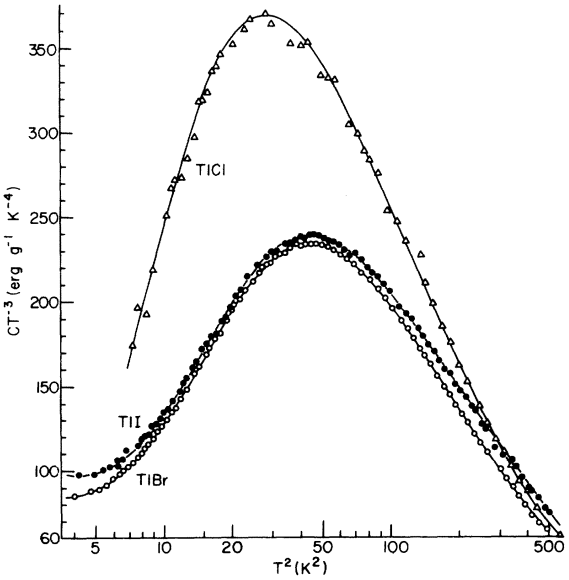

FIG. 1. CT^{-3}-vs-T^2 plots for the thallous halides. The TlCl and TlBr samples were single crystals, TlI, a ceramic. All three solids are paraelectrics.

tures low enough to freeze out the Einstein oscillators (the way in which the data are plotted gives the illusion that this contribution may be larger than the Einstein-mode contribution to the specific heat, but this is not the case). This feature is much too large to be attributable to the experimental method. The domain-wall contribution immediately comes to mind for these ferroelectrics, and we shall return to this below.

III. EINSTEIN MODES

In this section we consider the Einstein frequencies associated with the data in Figs. 1–5.

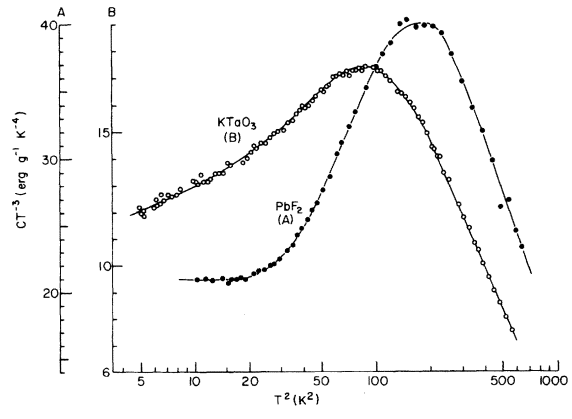

FIG. 2. CT^{-3}-vs-T^2 plots for cubic PbF_2 and $KTaO_3$. Both samples were single crystals and are paraelectrics. Designations A and B refer to the CT^{-3} scales.

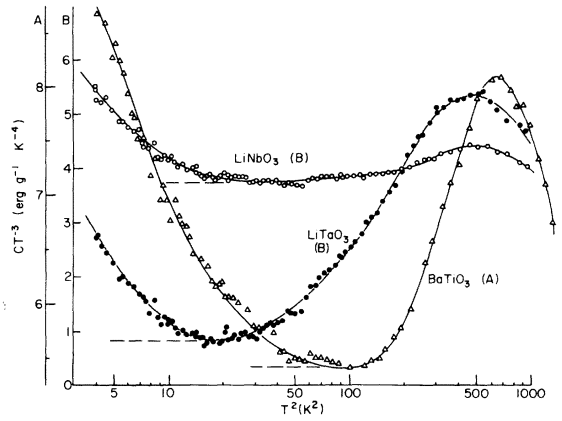

FIG. 3. CT^{-3}-vs-T^2 plots for the ferroelectrics $LiNbO_3$, $LiTaO_3$, and $BaTiO_3$, all of which were single-crystal, multidomain samples. No attempt was made to prepole the samples. Note the minima in CT^{-3}. Designations A, B, C refer to the CT^{-3} scales.

It is usual in these types of analyses to express the specific heat as a Debye term for the acoustic modes and Einstein terms for the optic modes. For example, Pandey[15] analyzed the specific heat of TiO_2 using three optic modes at 77 cm^{-1} (obtained from a force-constant model) and 143 and 189 cm^{-1} (infrared and Raman active). Sandin and Keesom[16] report 83 cm^{-1} for the lowest-frequency optic mode in TiO_2.[17] Five Einstein frequencies were used in the analysis in Ref. 9 for lithium sulfate monohydrate.

We will assume that for the temperatures involved here only the lowest-frequency mode contributes significantly, so that

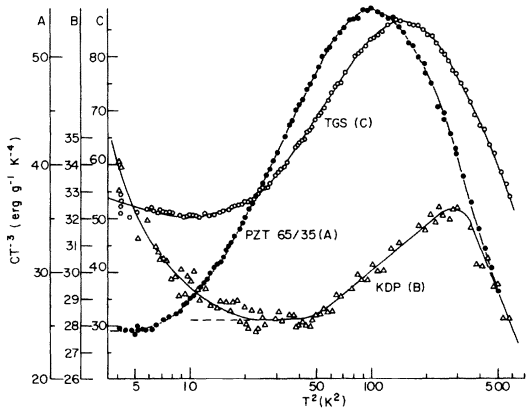

FIG. 4. CT^{-3}-vs-T^2 plots for the ferroelectrics TGS, KDP, and PZT 65/35. The TGS and KDP samples were multidomain single crystals, PZT 65/35, a hot-pressed ceramic. Note the CT^{-3} minima for TGS and KDP. No attempt was made to prepole the samples. Designations A, B, C refer to the CT^{-3} scales.

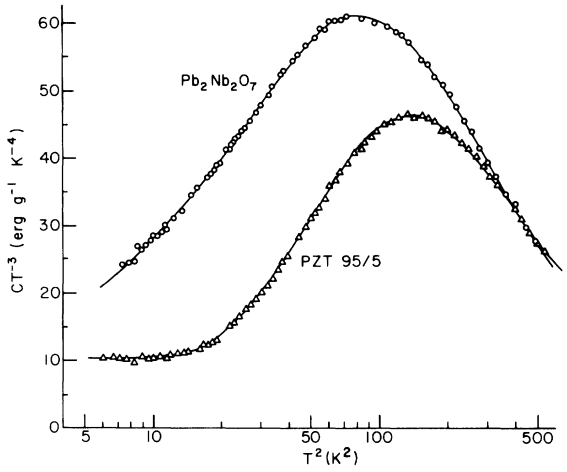

FIG. 5. CT^{-3}-vs-T^2 plots for antiferroelectric ceramic samples of $Pb_2Nb_2O_7$ and PZT 95/5.

$$C_{\text{expt}} = C_D(\Theta_D, T) + 3Rr\, x^2 e^x (e^x - 1)^{-2}, \qquad (2)$$

where C_D is the Debye term, Θ_D the Debye temperature, R the universal gas constant, r the number of atoms per formula weight contributing to the Einstein term, and $x = h\nu_E/kT$.

A three-level fitting scheme was used to determine Θ_D, r, and ν_E from the data in Figs. 1–5. For the ferroelectrics in Figs. 3 and 4, only those data for temperatures above the CT^{-3} minima were curve fitted, as indicated by the dashed lines in the figures. The assumption here is that the CT^{-3} minimum represents the acoustic "background" (see below). The fitting scheme was facilitated by selecting the initial value of ν_E from $T_{\max}$, Θ_D from the CT^{-3} minimum (or from the Lindemann equation),[18] and r from the low-temperature approximation to Eq. (2). Tabulated values of the Debye function were used, and the Debye temperatures given below result from curve fittings to the Debye function.

The results of these curve fittings are shown in Figs. 6–9, where the solid curves are drawn using the fitted data for Θ_D, ν_E, and r given in Table I (for clarity in plotting, the materials in Figs. 6–9 are not grouped as in Figs. 1–5). The low-temperature form of Eq. (2) is used for plotting in these figures—i.e., $\ln[T^2(C_{\text{expt}} - D_{\text{Debye}})]$ vs T^{-1}—and the curvatures at low T^{-1} values result from the full form, Eq. (1).

The data in Figs. 6–9 show remarkable agreement with Eq. (2) over many orders of magnitude. In all cases, the differences between the experimental and calculated values of CT^{-3} are $\lesssim \pm 5\%$, the approximate uncertainty in the measurements (the scatter in the points at large T^{-1} values is due to the very small differences between C_{expt} and C_{Debye}).

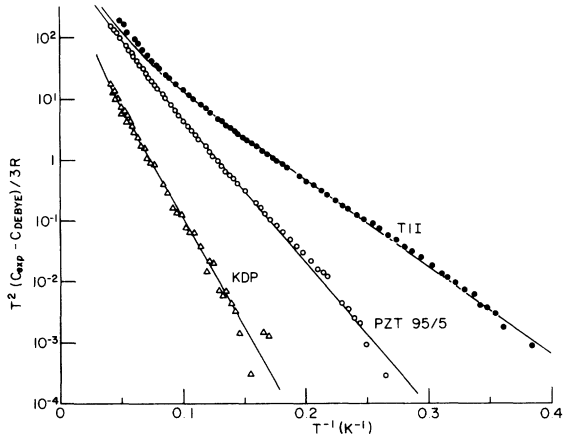

FIG. 6. Results of fitting the KDP, PZT 95/5, and TlI specific-heat data to Eq. (2). The Debye temperature which enters $T^2(C_{\text{expt}} - C_{\text{Debye}})$ was one of the fitting parameters. The solid curves were drawn using the fitted-parameter data, Table I, and the curvature at low T^{-1} results from using the complete expression for the Einstein term, Eq. (2). For the ferroelectrics, the specific-heat data at temperatures *above* the CT^{-3} minima were fitted.

The fitting results are summarized in Table I. Also given in Table I is the ratio of the number of Einstein modes, N_E, to the Debye modes, N_D, estimated from[2] $N_E/N_D = r(k\Theta_D/h\nu_E)^3$. As with the hexagonal tungsten bronzes,[2] the Einstein modes dominate the phonon spectra in these materials with the exceptions of $LiNbO_3$ and KDP.

IV. DISCUSSION

A. Paraelectrics

The Debye temperatures for the thallous halides are in reasonable agreement with predictions

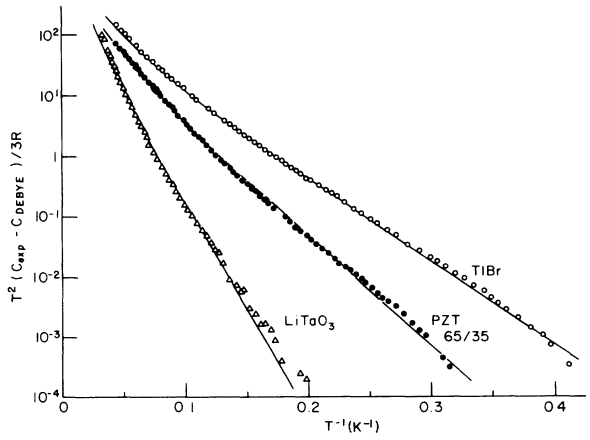

FIG. 7. Same as Fig. 6, for $LiTaO_3$, PZT 65/35, and TlBr.

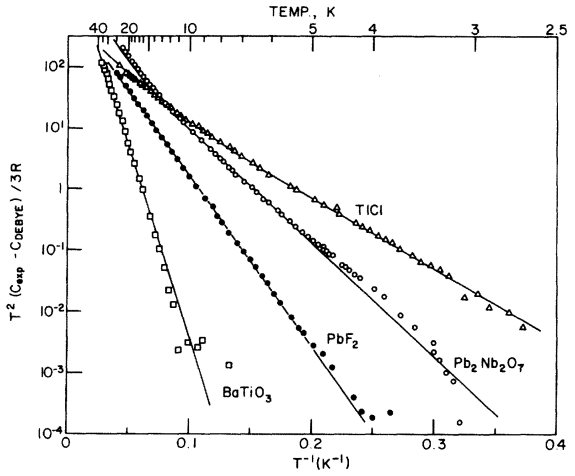

FIG. 8. Same as Fig. 6, for $BaTiO_3$, PbF_2, $Pb_2Nb_2O_7$, and TlCl.

TABLE I. Einstein modes in paraelectrics, ferroelectrics, antiferroelectrics.

Material	Θ_D (K)	Θ_E (K)	ν_E (cm^{-1})	r	N_E/N_D
TlCl	84.4	27.1	18.8	0.220	6.61
TlI	81.9	34.0	23.6	0.355	4.97
TlBr	90.7	32.3	22.4	0.274	6.10
PbF_2	156.2	63.0	43.8	0.217	3.30
$KTaO_3$	182.0	37.9	26.4	0.0131	1.45
$LiNbO_3$	327.3	114.0	79.3	0.0237	0.560
$LiTaO_3$	449.1	87.9	61.0	0.130	17.3
$BaTiO_3$	252.5	142.9	99.3	0.339	1.88
TGS	104.0	67.5	46.9	0.786	2.86
PZT65/35	129.8	45.5	31.6	0.172	3.98
KDP	172.0	85.8	59.6	0.0756	0.607
$Pb_2Nb_2O_7$	99.7	43.5	30.2	0.418	5.01
PZT95/5	172.0	54.9	38.1	0.394	12.2

from the Lindenmann relation,[18] 105, 82, and 96 K for TlCl, TlI, and TlBr, respectively. From room-temperature elastic-constant data,[19] the calculated Debye temperatures for TlBr and TlCl (which are cubic) are 115 and 125 K, respectively.[20] The specific-heat data on TlBr in Fig. 1 are in good agreement with the data of Brade and Yates,[7] who report effective Debye temperatures between 65 and 90 K in the range 5–20 K. The TlCl and TlI data in Fig. 1 agree well with other published measurements[7] in the overlap regions.

The frequency distribution in TlBr has been calculated by Cowley and Okazaki[21] by fitting various models to neutron dispersion data. A sudden, model-independent increase in the density of states was calculated at ≈ 0.7 THz $= 23$ cm^{-1}, which agrees well with the Einstein frequency in Table I, $\nu_E = 22.4$ cm^{-1}. This is analogous to the case of the superconductor TaC[3] mentioned above.

For TlCl, the low Einstein frequency (18.8 cm^{-1}) leads to an enormous specific heat. Though not shown in Fig. 1, the specific heat of this crystal was found to be independent of electric field strengths up to 13.6 kV/cm, which indicates that the Einstein frequency corresponds to acoustic phonons. A similar result was found in the hexagonal tungsten bronze Tl_xWO_3 ($\nu_E = 26.4$ cm^{-1}).[2] The vibrational spectrum of TlCl has been calculated by Kamal and Mendiratta[22] according to a shell model making use of elastic-constant data (i.e., acoustic modes) to evaluate short-range interaction parameters. Their calculated first phonon anomaly in the density of states occurs at ≈ 6 THz $= 200$ cm^{-1}. Neutron scattering data would be needed to clarify the phonon spectra of this material.

The Debye temperature for PbF_2 in Table I agrees reasonably well with the Lindemann-relation prediction, 140 K, but not with the calculation[20] based on room-temperature elastic-constant data,[23] 224 K.

Cubic PbF_2 is a paraelectric similar to the thallous halides[24]; the dielectric constant follows a Curie-Weiss behavior below room temperature but then flattens at a constant value at low temperatures and no phase transition to an ordered state takes place. The soft-mode frequency in PbF_2 is ≈ 100 cm^{-1} at room temperature, decreasing to ≈ 95 cm^{-1} at low temperatures.[24] Infrared reflectance measurements[25] on PbF_2 at room temperature reveal no phonon anomalies below 200 cm^{-1}, indicating that the 44-cm^{-1} mode is not infrared active.

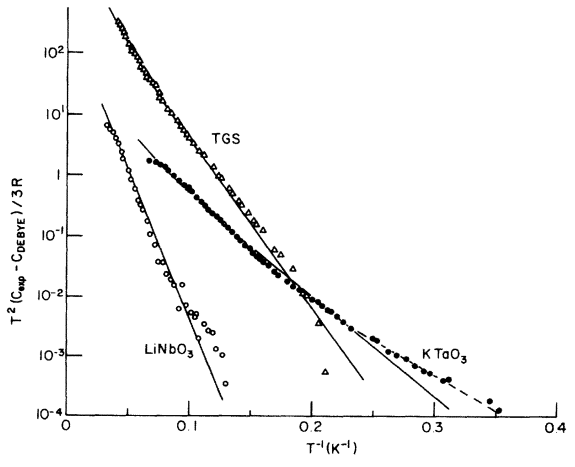

FIG. 9. Same as Fig. 6, for $LiNbO_3$, TGS, and $KTaO_3$. For $KTaO_3$, note the curvature of the data reflecting the temperature dependence of the soft mode. The solid curve through the $KTaO_3$ points represents $\nu_E = 26$ cm^{-1}, the dashed curve at large T^{-1} values, $\nu_E = 19$ cm^{-1}.

The Debye temperature for $KTaO_3$ in Table I is considerably smaller than the value calculated[20] from the room-temperature elastic constants,[26] 580 K, but larger than the Lindemann estimate, 147 K.

$KTaO_3$ remains paraelectric down to at least 2 K,[27] and it has been well established by Raman[28] and infrared[29] measurements that this paraelectric behavior is due to the softening of an underdamped, transverse-optic mode. The light scattering and dielectric measurements[30] are in very good agreement, and Samara and Morosin[30] give $\epsilon\omega_s^2 = 1.81 \times 10^6$ cm^{-2}, connecting the dielectric constant and the frequency of this mode according to the Lyddane-Sachs-Teller relation. Accordingly, at 3 and 25 K we expect $\omega_s = 22$ and 37 cm^{-1}, respectively, based on the dielectric data.[30] The Einstein data in Fig. 9 cover the range 3–25 K and yield $\nu_E = 26.4$ cm^{-1} (Table I) for the average frequency of this mode in this temperature range. The neutron data[31] yield 25–29 cm^{-1} for the soft mode in this temperature range. Some softening of this mode is evident in Fig. 9 from the departure of the data from the solid curve (the dashed curve for $KTaO_3$ in Fig. 9 at the lowest temperatures corresponds to $\nu_E \approx 19$ cm^{-1}).

The neutron data[31] show that this TO mode is almost degenerate with the LA mode over a considerable region of q space around 10 K. This mixture of modes was also seen in the specific-heat measurements: The field dependence of the specific heat of $KTaO_3$ up to 15.6 kV/cm is considerably weaker than one would expect if ν_E were due entirely to the soft mode.[32]

Pronounced line broadening for the TA modes in $KTaO_3$ at 4 K compared to 28 K has led to the suggestion[31] that a "small" phase transition at 10 K has taken place due to the interaction of the soft mode with the LA mode. A similar effect has been observed in $SrTiO_3$,[33] and specific-heat measurements on $SrTiO_3$ near 106 K have revealed this transition.[34] Our data here reveal no such transition in $KTaO_3$ at 10 K (note that at 10 K a phase-transition specific-heat anomaly would be much more pronounced than at 106 K).

B. Ferroelectrics

The Debye temperature for $LiTaO_3$ in Table I, 449 K, agrees well with other measurements,[35] $\Theta_D = 450$ K, but the $LiNbO_3$ result here, 327 K, is not in agreement with other measurements,[36] $\Theta_D = 560$ K.

$LiNbO_3$ and $LiTaO_3$ undergo ferroelectric phase transitions at elevated temperatures, 1210 and 665 °C, respectively. The soft mode is in both crystals an A_1-symmetry transverse-optic mode ($q \to 0$) whose frequency increases from near zero at the transition temperature to in excess of 200 cm^{-1} as $T \to 0$ K.[37] In addition, there are E-symmetry optic modes which have lower excitation energies than the $q \approx 0$ A_1 mode. These E modes were initially reported to be at 90 cm^{-1} in $LiNbO_3$ and 70 cm^{-1} in $LiTaO_3$ based on Raman data.[37] However, more recent measurements[38] placed these modes at 150 and 140 cm^{-1}, respectively. The Table I data for $LiNbO_3$ (79 cm^{-1}) and $LiTaO_3$ (61 cm^{-1}) favor the original Raman data, although these specific-heat modes can occur anywhere in the Brillouin zone.

Recent measurements[39] of the pyroelectric response of $LiNbO_3$ and $LiTaO_3$ could be explained assuming low-energy optic modes with minimum energy gaps ($\omega_q \to 0$) of 67 and 63 cm^{-1}, respectively. These authors had difficulty explaining their pyroelectric-response data above ≈30 K for $LiNbO_3$ using $\Theta_D = 560$ K.[36] The lower Θ_D reported here for $LiNbO_3$ would improve the comparison of these data.

The Debye temperature for $BaTiO_3$ in Table I, 252.5 K, is larger than the Lindemann prediction (≈170 K) but almost one-half the value estimated from (cubic) elastic-constant data, 477 K.[40] At the temperatures involved here, $BaTiO_3$ is rhombohedral, having undergone three phase transitions (cubic → tetragonal → orthorhombic → rhombohedral). It is not clear how the acoustic spectrum could be altered considerably by these transitions, which involve relatively minor shears in the unit cell. A similar discrepancy between the elastic and calorimetric Debye temperatures was seen above for $KTaO_3$.

An overdamped transverse-optic mode at 35 cm^{-1} has been observed at 300 K in tetragonal $BaTiO_3$,[41] and Raman studies place the lowest longitudinal-optic mode at 180 cm^{-1} at this temperature.[42] The 99.3-cm^{-1} mode (Table I) may correspond to the lowest optic mode in the rhombohedral phase.

The Debye temperature for KDP in Table I agrees reasonably well with the value estimated from low-temperature thermal-conductivity data,[43] ≈195 K. The elastic-constant data for paraelectric KDP yield 237 K for the Debye temperature.[44] A literature survey[45] did not reveal any thermal data on TGS.

The hydrogen-bonded ferroelectrics, KDP and TGS, involve more-complex phonon properties than the displacive ferroelectrics ($BaTiO_3$, $KTaO_3$, etc). The onset of ferroelectricity in these materials entails proton displacements on oxygen-oxygen bonds which are coupled to phonon modes involving the other ions. In KDP, there is piezoelectric coupling between optic and acoustic

modes in the paraelectric phase (noncentrosymmetric point group $42m$). Raman, Brillouin, and infrared measurements have been made on these two ferroelectrics in the paraelectric phases and have been summarized elsewhere.[6] An underdamped soft mode at ≈ 100 cm^{-1} has been observed in the ferroelectric phase of KDP at 85 K.[6]

The PZT 65/35 ceramic (and PZT 95/5) belongs to the system $Pb(Zr_xTi_{1-x})O_3$, which has received considerable recent attention for piezoelectric and electro-optic applications. At room temperature, four PZT phases exist: tetragonal ferroelectric ($x < 0.53$), rhombohedral ferroelectric FE_2 ($0.53 < x < 0.63$), rhombohedral ferroelectric FE_1 ($0.63 < x < 0.94$), and orthorhombic antiferroelectric ($x > 0.94$). (This nomenclature, FE_1 and FE_2, is used to denote the two rhombohedral ferroelectric phases of these ceramics.)

Raman spectra have been measured at room temperature on these ceramics for[46] $x < 0.35$ with the following results: (i) The frequency of the soft E(TO) varies roughly as $x^{1/2}$ from 89 cm^{-1} at $x = 0$ ($PbTiO_3$) to ≈ 0 cm^{-1} at the $x = 0.53$ morphotropic phase boundary between the tetragonal and rhombohedral FE_2 phases; (ii) the higher-frequency optic modes ($\gtrsim 200$ cm^{-1}) are independent of x; (iii) the E(TO) band broadens with increasing x, and compositions in both rhombohedral fields display broad featureless Raman spectra; (iv) the intensity of a broad band centered in the 50–60-cm^{-1} range grows with x and is believed associated with the large density of zone-boundary TA phonons observed in $PbTiO_3$ by neutron scattering measurements.

The PZT 65/35 ceramic is in the FE_1 field, where powder Raman methods are unable to resolve phonon symmetries and frequencies and single crystals are difficult to make for neutron studies. It is most likely that the $\nu_E = 31.6$ cm^{-1} (Table I) corresponds to the average frequency of the zone-boundary TA phonons in this ceramic at low temperatures.[47]

C. Antiferroelectrics

The PZT 95/5 ceramic is very close compositionally to $PbZrO_3$, but samples of $PbZrO_3$ suitable for neutron spectroscopy have not been available. The relative closeness of the ν_E's for $x = 0.65$ (32 cm^{-1}) and for $x = 0.95$ (38 cm^{-1}) leads one to suspect that the Einstein modes in both ceramics are due to the same zone-boundary TA phonons.[47]

Lead pyroniobate, $Pb_2Nb_2O_7$, was reported to be an antiferroelectric with a phase transition at 15.4 K,[48] but very little additional work appears to have been done on this material. An x-ray analysis indicated that the ceramic measured here had the pyrochlore structure, but as seen in Fig. 5 no anomaly is present in the specific heat at 15.4 K ($T^2 = 237$).[49] The specific-heat properties of this ceramic are quite similar to the lead zirconate titanates ($\Theta_D \sim 100$ K, $\nu_E \sim 30$ cm^{-1}).

D. Domain-wall contribution

The data in Figs. 3 and 4 for the ferroelectrics $LiNbO_3$, $LiTaO_3$, $BaTiO_3$, TGS, and KDP show *minima* in CT^{-3}, in contrast to the paraelectrics (Figs. 1 and 2) and antiferroelectrics (Fig. 5). Note that all materials were measured under identical conditions and that the addenda contributions were roughly equivalent (with the exception of $LiTaO_3$).

The increase in CT^{-3} with decreasing temperature at the lower temperatures for the ferroelectrics suggests a domain-wall contribution, and various common specific-heat functionals were attempted to fit these data below the CT^{-3} minima.

Remarkably high-accuracy fits were obtained for the form

$$C = AT^3 + BT^{3/2} \tag{3}$$

for $BaTiO_3$, $LiNbO_3$, TGS, and KDP.[50] These data are shown in Fig. 10, and the fitting informa-

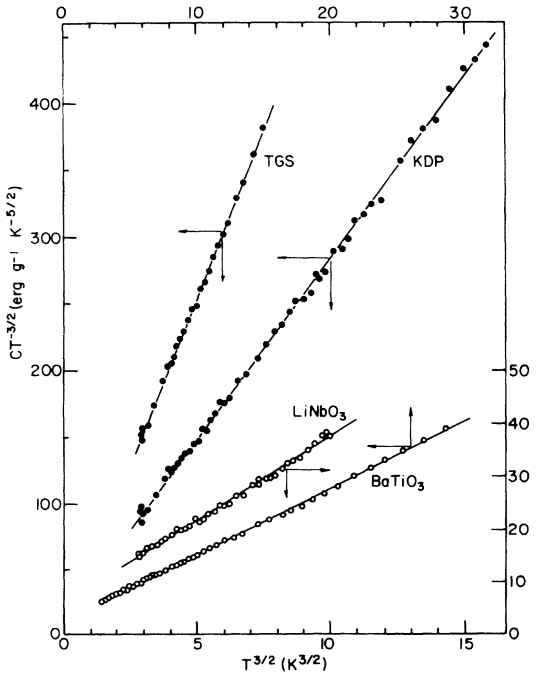

FIG. 10. $CT^{-3/2}$ vs $T^{3/2}$ for the ferroelectric crystals TGS, KDP, $LiNbO_3$, and $BaTiO_3$ for temperatures below the CT^{-3} minima of Figs. 3 and 4. The excellent fits reflected in Table II leave no doubt as to the presence of the $T^{3/2}$ term in Eq. (3) which is probably due to domain walls.

tion is summarized in Table II, where the Θ_D values are obtained from the coefficient A in Eq. (3), and confidence limits are given for the B coefficient.

The Θ_D values in Tables I and II are very close, indicating that the $T^{3/2}$ contribution does not introduce a significant error in determining the Einstein frequencies at the higher temperatures according to Eq. (2).

The case of $LiTaO_3$ appears pathological in that the data below the CT^{-3} minimum did not follow Eq. (3). The addenda corrections for this crystal were relatively large compared to the other samples, but it is not believed that the CT^{-3} data below the minimum can be explained as an addenda effect.

The specific-heat data for PZT 65/35, Fig. 4, do not extend to low enough temperatures to resolve a possible $T^{3/2}$ contribution.

An attempt was made to curve fit all the ferroelectric specific heats below the CT^{-3} minima according to Eq. (2)—i.e., Einstein-mode analyses. The fits obtained were considerably inferior to the $T^{3/2}$ fits shown in Fig. 10, although the $LiTaO_3$ data could be represented approximately by Eq. (2). The Einstein frequencies obtained from these fits varied from 2.9 cm^{-1} for $LiTaO_3$ to 5.1 cm^{-1} for $BaTiO_3$. Conceivably, a $T^{3/2}$ domain-wall contribution *plus* a low-lying Einstein mode are active in $LiTaO_3$, which would frustrate either analysis. Still-lower-temperature specific-heat measurements might clarify this material.

Spin waves in ferro- and ferrimagnetic materials contribute a $T^{3/2}$ specific-heat term.[51] In fact, the possibility of observing the analogous pseudo-spin-wave contribution in the hydrogen-bonded ferroelectrics first suggested the $T^{3/2}$ plot. In the case of these dielectrics, the presence of the $T^{3/2}$ term depends on whether the material is ferroelectric or not, rather than whether the ferroelectric is displacive or hydrogen bonded.

This strongly suggests a commonality in the domain-wall contribution to the low-temperature specific heat of ferroelectrics. It is possible to sketch the broad outline of how this contribution might arise along the following line: First, quantized waves which obey Bose-Einstein statistics contribute a $T^{3/2}$ or T^3 term to the specific heat depending on whether the dispersion relation follows $\omega \propto q^2$ (as for magnons in ferromagnets) or $\omega \propto q$ (as for low-frequency phonons and for magnons in antiferromagnets), respectively. Minute domain-wall displacements give rise to a force proportional to the displacement and tending to restore equilibrium, so that wall oscillations take place. If such wall oscillations can be quantized resulting in $\omega \propto q^2$, then a $T^{3/2}$ specific-heat term would follow.

TABLE II. $T^{3/2}$ fitting data for ferroelectrics.

Crystal	Θ_D (K)	B (erg g^{-1} $K^{-5/2}$)	Residual standard deviation in $CT^{-3/2}$
$BaTiO_3$	255	10.77 ± 0.12	0.86
$LiNbO_3$	347	6.03 ± 0.08	0.51
TGS	107	7.65 ± 0.48	2.4
KDP	175	15.40 ± 0.50	3.6

V. CONCLUSIONS

A relatively large amount of new, low-temperature specific-heat data have been presented in this paper on ferroelectric-type solids which, for the most part, have been studied extensively at higher temperatures by other experimental methods. The dielectric activity in these solids is known to be intimately related to low-lying vibrational levels which we have tried to correlate with Einstein frequencies from the calorimetric data, where possible. The specific heat, of course, involves integration over the density of states so that the mode assignments can only be inferred.

The specific heats of these solids show a rather surprising amount of structure in the CT^{-3} plots, and excellent data fits are obtained for all materials using single Einstein frequencies. Where possible, the Einstein frequencies agree well with the positions of phonon anomalies determined from scattering experiments—e.g., TlBr and $KTaO_3$.

The PZT specific-heat data provide information on the experimentally inaccessible rhombohedral ferroelectric and orthorhombic antiferroelectric phases, and the evidence discussed above points to low-frequency TA modes in these ceramics at ≈ 35 cm^{-1}.

It is not clear why there are such large discrepancies between the calorimetric and elastic-constant Debye temperatures for $KTaO_3$ and $BaTiO_3$. Elastic-constant data are measured at higher temperatures in the cubic phase, and, on the other hand, a soft optic mode at lower temperatures will depress acoustic branches. Specific-heat data at even lower temperatures would shed light on this problem.

The $T^{3/2}$ domain-wall contribution is an interesting effect discovered from these measurements. Further work would be enlightening here. It would be expected that the B coefficient in Eq. (3) would depend on the number of domain walls present in the crystal which can be controlled by poling at higher temperatures. Along this line,

the demonstration of a $T^{3/2}$ pseudo-spin-wave contribution in the hydrogen-bonded ferroelectrics would be a direct confirmation of the pseudo-spin-wave theory, which suffers from lack of direct experimental contact at higher temperatures (in fact, well-defined pseudo-spin-waves exist only at low temperatures). Our findings here demonstrate that the domain-wall contribution can mask the pseudo-spin-wave contribution, which means that the experiment would have to be carried out on a single-domain crystal of KDP or TGS.

ACKNOWLEDGMENTS

It is a pleasure to acknowledge the hospitality of the Cryogenics Division of the NBS–Boulder, where these measurements were performed while the author was a Guest Worker. The crystals and ceramics, except for TGS and $Pb_2Nb_2O_7$, were kindly supplied by Dr. George Samara, and his interest in this work and comments on the manuscript are deeply appreciated. Thanks are also due Alan Morrow for preparing the $Pb_2Nb_2O_7$ ceramic and Mrs. Bernice Bender for assistance in the computer data handling.

[1]See the review article by A. J. Leadbetter, Phys. Chem. Glasses 9, 1 (1968).
[2]A. J. Bevolo, H. R. Shanks, P. H. Sidles, and G. C. Danielson, Phys. Rev. B 9, 3220 (1974).
[3]P. Roedhammer, E. Gmelin, and W. Weber, Solid State Commun. 16, 1205 (1975).
[4]Recently published calorimetric data on the semiconducting chalcopyrites and magnetic semiconducting chalcogenides reveal low-frequency modes ~ 30–80 cm^{-1} in these materials based on minima in the effective Debye temperatures, but the data were not analyzed for the ν_E's [S. C. Abrahams and F. S. L. Hsu, J. Chem. Phys. 63, 1162 (1975)].
[5]W. Cochran, Adv. Phys. 9, 387 (1960).
[6]J. F. Scott, Rev. Mod. Phys. 46, 83 (1974); R. Blinc and B. Zeks, *Soft Modes in Ferroelectrics and Antiferroelectrics* (Elsevier, New York, 1974).
[7]R. M. Brade and B. Yates, J. Phys. C 4, 417 (1971); Y. Takahashi and E. F. Westrum, Jr., J. Chem. Eng. Data 10, 244 (1965); I. R. Bartky and W. G. Giauque, J. Am. Chem. Soc. 81, 4169 (1959).
[8]E. Hegenbarth, Phys. Status Solidi 2, 1544 (1962). Recent measurements on $SrTiO_3$ down to 1.2 K will be published elsewhere [J. H. Colwell (private communication)].
[9]I. E. Paukov and M. N. Lavrenteva, Russ. J. Phys. Chem. 43, 775 (1969).
[10]J. E. Neighbor, Rev. Sci. Instrum. 37, 497 (1966).
[11]R. J. Corruccini and J. J. Gniewek, Monograph U. S. Natl. Bur. Stand. No. 21 (U.S. GPO, Washington, D.C., 1960); J. C. Ho, H. R. O'Neal, and N. E. Phillips, Rev. Sci. Instrum. 34, 782 (1963).
[12]J. L. Cude and L. Finegold, Cryogenics 11, 394 (1971); J. T. Heessels, Cryogenics 11, 483 (1971).
[13]Cryocal No. 3771.
[14]W. N. Lawless, Cryogenics 15, 273 (1975).
[15]H. N. Pandey, Phys. Status Solidi 11, 743 (1965).
[16]T. R. Sandin and P. H. Keesom, Phys. Rev. 177, 1370 (1969).
[17]Though not reported here, TiO_2 was also measured in this study and analyzed according to Eq. (2). The fitted Einstein frequency found was 82.2 cm^{-1}.
[18]The Lindemann equation relates θ_D to the melting temperature, density, and molecular weight; see Ref. 4.
[19]G. E. Morse and A. W. Lawson, J. Phys. Chem. Solids 28, 939 (1967); S. Haussuhl, Acta Crystallogr. 13, 685 (1960).
[20]H. Leadbetter (private communication).
[21]E. R. Cowley and A. Okazaki, Proc. R. Soc. A 300, 45 (1967).
[22]R. Kamal and R. G. Mendiratta, J. Phys. Soc. Jpn. 26, 621 (1969).
[23]J. H. Wasilik and M. L. Wheat, J. Appl. Phys. 36, 791 (1965).
[24]G. H. Samara, Ferroelectrics (to be published), and private communication.
[25]P. Denham, G. R. Field, P. L. R. Morse, and G. R. Wilkinson, Proc. R. Soc. A 317, 55 (1970).
[26]Measured by R. Reed and H. Leadbetter [U.S. Natl. Bur. Stand., Boulder (private communication)].
[27]Measurements on $KTaO_3$ down to 0.013 K reveal a small peak at about 2 K in the dielectric constant [J. C. Holste and W. N. Lawless (unpublished)].
[28]P. A. Fleury and J. M. Worlock, Phys. Rev. 174, 613 (1968).
[29]C. H. Perry and T. F. McNelly, Phys. Rev. 154, 456 (1967).
[30]G. A. Samara and B. Morosin, Phys. Rev. B 8, 1256 (1973). The $KTaO_3$ crystal measured here was the same one studied in this paper.
[31]G. Shirane, R. Nathans, and V. J. Minkiewicz, Phys. Rev. 157, 396 (1967).
[32]The field-dependent specific heat and electrocaloric properties of $KTaO_3$ are reported in another paper, W. N. Lawless (unpublished).
[33]R. A. Cowley, Phys. Rev. 134, A981 (1964).
[34]P. R. Garnier, Phys. Lett. 35A, 413 (1971).
[35]J. Marta, quoted in Ref. 39.
[36]J. Bergman, quoted in Ref. 39.
[37]W. D. Johnston and I. P. Kaminow, Phys. Rev. 168, 1045 (1968).
[38]A. S. Barker, A. A. Ballman, and J. A. Ditzenberger, Phys. Rev. B 2, 4322 (1970).
[39]A. M. Glass and M. E. Lines (unpublished).
[40]D. Berlincourt and H. Jaffe, Phys. Rev. 111, 143 (1958).
[41]P. A. Fleury and P. D. Lazay, Phys. Rev. Lett. 26, 1331 (1971); P. S. Peercy and G. A. Samara, Phys. Rev. B 6, 2748 (1972).
[42]A. Pinczuk, W. Taylor, E. Burstein, and I. Lefkowitz, Solid State Commun. 5, 429 (1967).
[43]Y. Suemune, J. Phys. Soc. Jpn. 22, 735 (1965).
[44]S. K. Joshi and S. S. Mitra, Proc. Phys. Soc. Lond. 76,

295 (1960).
[45]Prepared by the Cryogenic Data Center, Institute for Basic Studies, U. S. Natl. Bur. Stand., Boulder, 1975.
[46]R. Merlin and A. Pinczuk, Ferroelectrics 7, 275 (1974), and references quoted therein; and Ferroelectrics (to be published).
[47]Electric-field-dependent specific-heat measurements in progress on the PLZT series demonstrate that in PZT 65/35 and PZT 95/5, ν_E is independent of electric fields up to 40 kV/cm, further confirming the TA-mode assignment.
[48]J. K. Hulm, Phys. Rev. 92, 504 (1953).
[49]Field-dependent specific-heat, dielectric-constant, and polarization measurements now in progress rule out any phase transition in this material below 30 K [J. D. Siegwarth, W. N. Lawless, and A. J. Morrow (unpublished)].
[50]These unusual results were reported earlier. W. N. Lawless, Phys. Rev. Lett. 36, 478 (1976).
[51]E. S. R. Gopal, *Specific Heats at Low Temperatures* (Plenum, New York, 1966).